

Technical Report ARAEW-TR-07012

Chirp-Pulse Terahertz Range Profiling

Wei Liang¹
Jeffrey M. Warrender²
X.-C. Zhang¹

1. Terahertz Research Center, Rensselaer Polytechnic Institute, Troy, NY, 12180
2. U.S. Army Benét Laboratories

October 2007



ARMAMENT RESEARCH, DEVELOPMENT AND ENGINEERING CENTER
Armaments Engineering & Technology Center
Weapon Systems & Technology



Approved for public release; distribution is unlimited.

The views, opinions, and/or findings contained in this report are those of the author(s) and should not be construed as an official Department of the Army position, policy, or decision, unless so designated by other documentation.

The citation in this report of the names of commercial firms or commercially available products or services does not constitute official endorsement by or approval of the U.S. Government.

Destroy this report when no longer needed by any method that will prevent disclosure of its contents or reconstruction of the document. Do not return to the originator.

REPORT DOCUMENTATION PAGE				Form Approved OMB No. 0704-0188	
<small>Public reporting burden for this collection of information is estimated to average 1 hour per response, including the time for reviewing instructions, searching data sources, gathering and maintaining the data needed, and completing and reviewing the collection of information. Send comments regarding this burden estimate or any other aspect of this collection of information, including suggestions for reducing this burden to Washington Headquarters Service, Directorate for Information Operations and Reports, 1215 Jefferson Davis Highway, Suite 1204, Arlington, VA 22202-4302, and to the Office of Management and Budget, Paperwork Reduction Project (0704-0188) Washington, DC 20503.</small>					
PLEASE DO NOT RETURN YOUR FORM TO THE ABOVE ADDRESS.					
1. REPORT DATE (DD-MM-YYYY) 10/10/2007		2. REPORT TYPE Technical		3. DATES COVERED (From - To)	
4. TITLE AND SUBTITLE Chirp-Pulse Terahertz Range Profiling				5a. CONTRACT NUMBER	
				5b. GRANT NUMBER	
				5c. PROGRAM ELEMENT NUMBER	
6. AUTHOR(S) Wei Liang* Jeffrey M. Warrender** X.-C. Zhang*				5d. PROJECT NUMBER	
				5e. TASK NUMBER	
				5f. WORK UNIT NUMBER	
7. PERFORMING ORGANIZATION NAME(S) AND ADDRESS(ES) U.S. Army ARDEC Benet Laboratories, RDAR-WSB Watervliet, NY 12189-4000				8. PERFORMING ORGANIZATION REPORT NUMBER ARAEW-TR-07012	
9. SPONSORING/MONITORING AGENCY NAME(S) AND ADDRESS(ES) U.S. Army ARDEC Benet Laboratories, RDAR-WSB Watervliet, NY 12189-4000				10. SPONSOR/MONITOR'S ACRONYM(S)	
				11. SPONSORING/MONITORING AGENCY REPORT NUMBER	
12. DISTRIBUTION AVAILABILITY STATEMENT Approved for public release; distribution is unlimited.					
13. SUPPLEMENTARY NOTES *Terahertz Research Center, Rensselaer Polytechnic Institute, Troy, NY, 12180 **U.S. Army Benét Laboratories					
14. ABSTRACT Terahertz (THz) range profiling is investigated for several cm-size metal targets. Aperiodically-poled lithium niobate crystals are used to generate a chirp-pulse THz signal, which is used to probe several targets. The reflected waveforms from different targets show distinctive features that permit differentiation of the targets. Several additional research tasks required prior to implementation of this detection concept into a prototype system are identified.					
15. SUBJECT TERMS Terahertz (THz) range; chirp-pulse; waveforms; THz radiation range profile system					
16. SECURITY CLASSIFICATION OF:			17. LIMITATION OF ABSTRACT U	18. NUMBER OF PAGES 23	19a. NAME OF RESPONSIBLE PERSON Jeffrey Warrender
a. REPORT U/U	b. ABSTRACT U/U	c. THIS PAGE U/U			19b. TELEPHONE NUMBER (Include area code) 518-266-5128

INSTRUCTIONS FOR COMPLETING SF 298

1. REPORT DATE. Full publication date, including day, month, if available. Must cite at least the year and be Year 2000 compliant, e.g., 30-06-1998; xx-08-1998; xx-xx-1998.

2. REPORT TYPE. State the type of report, such as final, technical, interim, memorandum, master's thesis, progress, quarterly, research, special, group study, etc.

3. DATES COVERED. Indicate the time during which the work was performed and the report was written, e.g., Jun 1997 - Jun 1998; 1-10 Jun 1996; May - Nov 1998; Nov 1998.

4. TITLE. Enter title and subtitle with volume number and part number, if applicable. On classified documents, enter the title classification in parentheses.

5a. CONTRACT NUMBER. Enter all contract numbers as they appear in the report, e.g. F33615-86-C-5169.

5b. GRANT NUMBER. Enter all grant numbers as they appear in the report, e.g. 1F665702D1257.

5c. PROGRAM ELEMENT NUMBER. Enter all program element numbers as they appear in the report, e.g. AFOSR-82-1234.

5d. PROJECT NUMBER. Enter all project numbers as they appear in the report, e.g. 1F665702D1257; ILIR.

5e. TASK NUMBER. Enter all task numbers as they appear in the report, e.g. 05; RF0330201; T4112.

5f. WORK UNIT NUMBER. Enter all work unit numbers as they appear in the report, e.g. 001; AFAPL30480105.

6. AUTHOR(S). Enter name(s) of person(s) responsible for writing the report, performing the research, or credited with the content of the report. The form of entry is the last name, first name, middle initial, and additional qualifiers separated by commas, e.g. Smith, Richard, Jr.

7. PERFORMING ORGANIZATION NAME(S) AND ADDRESS(ES). Self-explanatory.

8. PERFORMING ORGANIZATION REPORT NUMBER. Enter all unique alphanumeric report numbers assigned by the performing organization, e.g. BRL-1234; AFWL-TR-85-4017-Vol-21-PT-2.

9. SPONSORING/MONITORS AGENCY NAME(S) AND ADDRESS(ES). Enter the name and address of the organization(s) financially responsible for and monitoring the work.

10. SPONSOR/MONITOR'S ACRONYM(S). Enter, if available, e.g. BRL, ARDEC, NADC.

11. SPONSOR/MONITOR'S REPORT NUMBER(S). Enter report number as assigned by the sponsoring/ monitoring agency, if available, e.g. BRL-TR-829; -215.

12. DISTRIBUTION/AVAILABILITY STATEMENT. Use agency-mandated availability statements to indicate the public availability or distribution limitations of the report. If additional limitations/restrictions or special markings are indicated, follow agency authorization procedures, e.g. RD/FRD, PROPIN, ITAR, etc. Include copyright information.

13. SUPPLEMENTARY NOTES. Enter information not included elsewhere such as: prepared in cooperation with; translation of; report supersedes; old edition number, etc.

14. ABSTRACT. A brief (approximately 200 words) factual summary of the most significant information.

15. SUBJECT TERMS. Key words or phrases identifying major concepts in the report.

16. SECURITY CLASSIFICATION. Enter security classification in accordance with security classification regulations, e.g. U, C, S, etc. If this form contains classified information, stamp classification level on the top and bottom of this page.

17. LIMITATION OF ABSTRACT. This block must be completed to assign a distribution limitation to the abstract. Enter UU (Unclassified Unlimited) or SAR (Same as Report). An entry in this block is necessary if the abstract is to be limited.

ABSTRACT

Terahertz (THz) range profiling is investigated for several cm-size metal targets. Aperiodically-poled lithium niobate crystals are used to generate a chirp-pulse THz signal, which is used to probe several targets. The reflected waveforms from different targets show distinctive features that permit differentiation of the targets. Several additional research tasks required prior to implementation of this detection concept into a prototype system are identified.

Table of Contents

Abstract	i
Table of Contents	ii
List of Figures	ii
Introduction	1
Background	1
Experimental Details	5
Experimental Data	11
Discussion	18
Conclusion	19
Acknowledgement	20
References	20

List of Figures

Figure 1: Coordinates system; two aspect angles are defined	2
Figure 2: Formation of a range profile from a collection of point scatterers from the target	3
Figure 3: A chirp waveform. (a) envelope; (b) frequency; (c) waveform	3
Figure 4: A convolution example.....	4
Figure 5: Schematic of aperiodically poled Lithium Niobate (AppLN) domain structure.....	6
Figure 6: Schematic diagram of a THz-TDS used in the THz range profile measurement.....	7
Figure 7: (a) Experimental electric field amplitude of AppLN sample comparable to those used in this work. (b) Corresponding wavelength dependence vs. time; the pulse is “chirped” as desired	7
Figure 8: Waveform for AppLN sample b, nominal frequency range: 300-500GHz.....	8
Figure 9: FT spectrum of sample b. The DC component is removed.....	9
Figure 10: Sample a waveform	9
Figure 11: Sample a spectrum.....	10
Figure 12: "Wedding cake" sample schematic	11
Figure 13: 'Wedding cake' sample response	12
Figure 14: Average response of 'wedding cake' sample, as compared to the reference signal	12
Figure 15: Difference between "wedding cake" and reference signals, from Fig. 14	13
Figure 16: Pictures of targets used in the experiments	14
Figure 17: Reference signal after matched-filter by itself	14
Figure 18: Signal from sample 'Square block'	15
Figure 19: Signal from sample 'Al block & washer'	15
Figure 20: Waveform comparison between two samples: a collection of hex nuts (blue waveform) and a washer (red waveform)	16
Figure 21: Waveform of 3-coin target	16

List of Figures (Continued)

Figure 22: Zoomed-in view of the 3-coin waveform of Fig. 21 for the region to the left of the
blue vertical line..... 17

Figure 23: 3-sample comparison..... 18

INTRODUCTION

In this work, chirp-pulse terahertz (THz) range profile technology is investigated as a means to extend high resolution range profiling, commonly used in radar technology, into the THz regime. The ultimate goal of the project is the development of a device that is able to identify targets from a standoff distance in the battlefield or other hostile environments. This technology can also be readily adapted to other concealed weapon or explosive device detection scenarios.

Radar is most commonly used to identify a distant object. A powerful radio-frequency pulse is reflected off of the target and the reflected signal from the target forms a specific signal pattern at the receiver. This is due to the multiple reflective facets of the target along the radar direction and the target orientation. The signal is called a range profile. Different targets have different characteristic range profiles, thus a library for targets of interest can be constructed. By comparing with the library, a recognition algorithm can produce automatic target identification (ATI).

The technical difficulty of radar range profiling arises from the conflicting requirements for the radar power and spatial resolution. High spatial resolution requires short radar pulse duration, but short radar pulses may not carry enough power to have an acceptable signal-to-noise ratio. A chirped radar waveform is utilized to overcome these difficulties. Typical radar is operated at 1-10GHz frequency, 1 μ s-10ms pulse duration with peak power of 10kW.¹

The THz analogue of range profiling presents different challenges. The spatial resolution is much higher (mm range); this creates detection challenges because the temporal separation is now on the order of picoseconds instead of microseconds. Detection of the signal with electronic devices, such as the matched-filters that are used in radar detection, is impractical here because electronic equipment cannot respond on ps timescales. As a result, the use of a delay stage is required to obtain the waveform profile. It usually takes minutes to finish the target scan with an acceptable signal to noise ratio (S/N). This is antithetical to the goal of making a real-time measurement. In the terahertz research lab at RPI, a fast scanning delay stage has been demonstrated to finish the scan of a target of about 10cm in depth within 2 seconds, but this results in a degradation of 2-5 times in the S/N. A different approach, involving a single-shot measurement^{2,3} technology, can also be considered to make the measurement on an acceptable timescale.

BACKGROUND

For compactness, we restrict the following overview of radar range profiling to the case of a motionless target only. A schematic is shown in Fig. 1. Target identification is dependent upon the conventional angles of the target with respect to the radar source, namely, the aspect angle θ^a and elevation angle θ^e , where the vector \mathbf{s} is the radar propagation direction (the return signal $-\mathbf{s}$ is drawn).

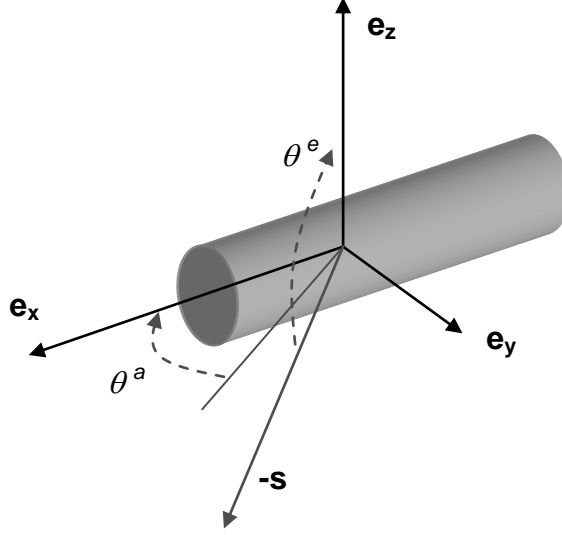


Fig. 1: Coordinates system; two aspect angles are defined.

From the radar receiver's point of view, a target consists of a collection of scatterers that reflect the radar pulse. Different locations of the scatterers generate returned radar echoes at different delay times. The collected signal of these echoes is the range profile of a target. Fig. 2 illustrates this concept. Measuring a target's reflectivity as a function of frequency over a given bandwidth gives equivalent information to measuring the target's reflectivity as a function of time delay⁴, and radar instrumentation often operates in the frequency domain because of this fact. The signal's bandwidth β is important because it determines the range resolution Δr , according to

$$\Delta r \approx \frac{c}{2\beta}, \quad (1)$$

where c is the speed of light. Frequency-domain measurements are generally made using a chirp-pulse. Such a pulse is characterized by a frequency that increases over the duration of the pulse, such as is shown in Fig. 3. Although the frequency shift can be linear, as shown in Fig. 3, more commonly, the pulse is increased in a step-wise fashion, with a uniform frequency step Δf . This permits several cycles of each frequency to be recorded, which sufficiently approximates a steady-state signal. The other advantage of the chirp-pulse is that a larger total bandwidth and pulse energy can be delivered. By equation (1) above, a higher bandwidth results in improved spatial resolution. The frequency step Δf sets the overall size of the target that can be investigated, R_{\max} , by

$$R_{\max} = \frac{c}{2\Delta f}. \quad (2)$$

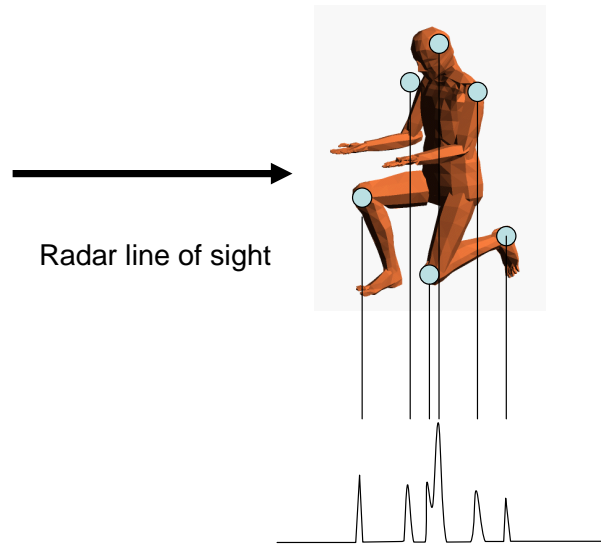


Fig. 2: Formation of a range profile from a collection of point scatterers from the target.

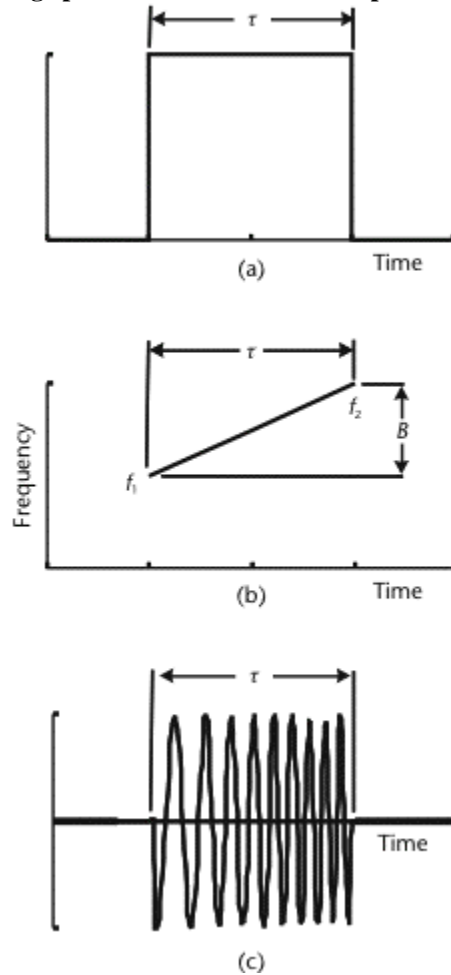


Fig. 3: A chirp waveform. (a) envelope; (b) frequency; (c) waveform.

The returned radar signal is measured by a matched filter. The output of the filter is essentially a time convolution of the returned signal with the reference signal. The peak of the output indicates the exact time when the signal is reflected off the target and hit the receiver. Fig. 4 shows the result for a square pulse.

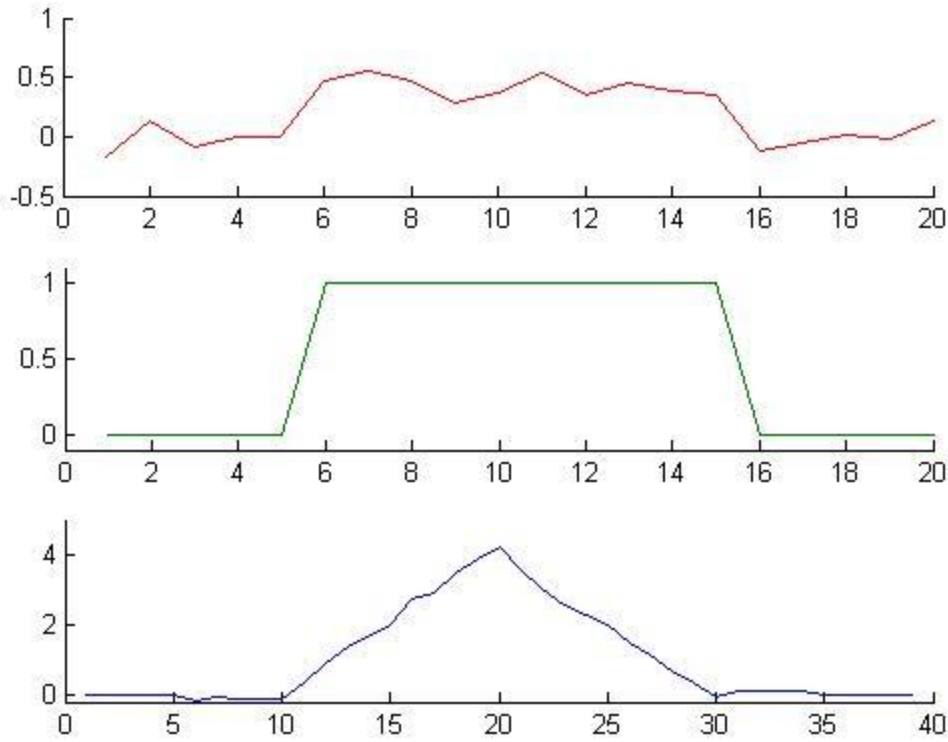


Fig. 4: A convolution example, (upper) a noise corrupted signal, reflected back from target; (middle) reference signal, emitted towards the target; (bottom) convolution signal after matched filter.

When this approach is applied to a chirped waveform, the reference signal at the receiver is one of the monotonic frequencies, e.g., f_l , the very first cycle in Fig. 3 (c); the reference signal does not match the other frequency component due to orthogonality but only the first cycle of signal waveform. From Fig. 3 (b), we know exactly where component f_l is situated within a pulse, hence a time resolution much smaller than the pulse duration τ is achieved. The duration of a chirp pulse is somewhat greater than the equivalent size of a target.

Radar pulse signals can be obtained electronically. For the chirped radar pulse, different frequency components of the pulse are individually matched by reference frequency signal and then sampled and recorded. This is a frequency domain measurement. An inverse Fourier Transform is performed on the signal to obtain a time domain range profile. Since the radar pulse duration is 10ms or shorter, the system responds to a target essentially in real time.

THz pulse detection, on the other hand, is based on the electro-optic effect. A femtosecond (fs) probe laser pulse sweeps the whole range of THz waveform in a nonlinear crystal, such as ZnTe. This causes an instantaneous birefringence change in the material, and the change is observed by monitoring a probe laser's signal in a balanced detector.⁵ For THz detection, the sweep is completed by sequential delay of probe laser pulse, usually *via* a mechanical delay stage. The stage moves stepwise, and a 5 μm distance corresponds to 33 femtoseconds temporal delay, the time needed for light traveling in round trip. The picosecond temporal scale is beyond the limit of electronic sampling, as no electronic device can respond on such a short time scale. However, THz pulse detection is a time-domain measurement. If it can be made in a timely fashion, there is no need for the synthesizing process (i.e., the Fourier transform) required when making a frequency domain measurement.

EXPERIMENTAL DETAILS

THz Time Domain Spectroscopy (THz-TDS) is an established technique for measuring a material's absorption or reflection spectrum. As a pump-probe technique, TDS involves illuminating the target with a THz beam and then using a probe beam to analyze how the material responds to the change to the reflected, or transmitted beam. A Ti:Sapphire optical oscillator laser beam (MIRA 900), of wavelength 800 nm, power 512 mW, pulse frequency 76 MHz, having a pulse duration of about 100 femtoseconds (fs) is separated into two beams by a beam splitter. The pump beam is incident upon a nonlinear optical crystal, such as ZnTe or LiNbO₃. A broadband THz pulse is emitted from the ZnTe, and is reflected off of the target. The reflected signal is sent via a system of parabolic mirrors into another crystal, the detector, which is typically ZnTe. The probe beam is passed through a mechanical delay stage, and then directed into the detector crystal collinearly with the THz beam. The THz beam causes a nonlinear optical process in the detector whereby the probe beam's polarization is rotated as it passes through the detector. The probe beam's polarization is split into s- and p- components, and these are sent into a pair of photodetectors, which are used to analyze the relative signal of the two polarizations. This arrangement is referred to as a balanced detector. To separate the signal from the noisy spectral background, the pump beam is chopped at 2377 Hz, and the photodetectors are connected to a lock-in amplifier which records measurements at this same frequency. The lock-in amplifier used here had a time constant of 300 ms.

We modified the conventional THz-TDS setup slightly to permit the delivery of a chirped pulse. Previously reported research has demonstrated that a chirped THz beam can be generated by passing a femtosecond laser pulse through an aperiodically poled Lithium Niobate (AppLN) crystal.⁶⁻⁹ Such a crystal has LN domains of alternating signs of the second order susceptibilities $\chi^{(2)}$, with the domain spacing increasing in size from one end of the material to the other. A schematic of the domain structure is shown in Fig. 5. When optical light traverses a material such as LN, a nonlinear optical effect called Optical Rectification creates a polarization across the material. By orienting domains with alternating opposite signs of nonlinear coefficient $\chi^{(2)}$, and by selection of a domain width that is comparable to the propagation time difference between the optical and THz pulse,¹⁰ a THz wave form will be generated that maps the domain structure. This was

originally utilized for probing the domain structure of ppLN crystals⁷, but the potential to create THz radiation of a single frequency, as opposed to the broadband radiation that results from electro-optic materials such as ZnTe, can be seen to have advantages for certain applications. Extending the concept further to the delivery of a chirped pulse further shows the versatility of this technique for THz pulse-shaping.

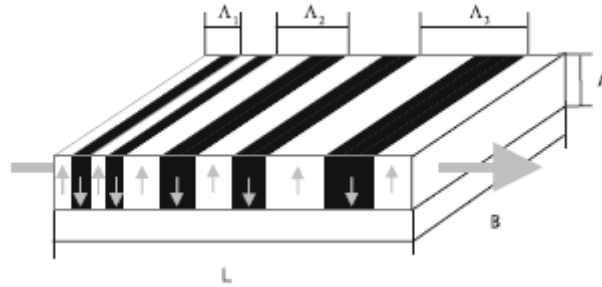


Fig. 5: Schematic of a periodically poled Lithium Niobate (AppLN) domain structure. From Ref. 9.

Two AppLN samples were used in this project. One gives a frequency range from 0.3-0.5 THz, and is referred to as “Sample b”; the other gives frequency range from 0.5-5 THz and is referred to as “Sample a”. Each sample is 5×5×0.5mm. The sample is mounted vertically, while the pump beam has horizontal polarization. The pump beam is focused into one side of the sample, a spot no larger than 0.3mm in diameter. THz radiation is emitted from the opposite side. LN is known to strongly absorb THz radiation, and a surface-emitting experimental geometry has been explored⁹ as a means of limiting the path length of the THz radiation within the LN, but this was not investigated during this study.

The mechanical delay stage is varied over a range of positions on the order of a few mm, which corresponds to a delay of several picoseconds (ps). In an ordinary THz-TDS measurement, this corresponds to sampling over the full range of the THz pulse. Here, the use of a pulse of chirped frequency gives a slightly different meaning to the action of the delay stage; the stage now can be thought to be sampling the various frequency components of the beam. This is analogous to the sampling that occurs in a radar measurement, with the exception that the short timescales inherent to THz equipment require electro-optic sampling rather than electronic sampling. A schematic of our experimental setup is shown in Fig. 6.

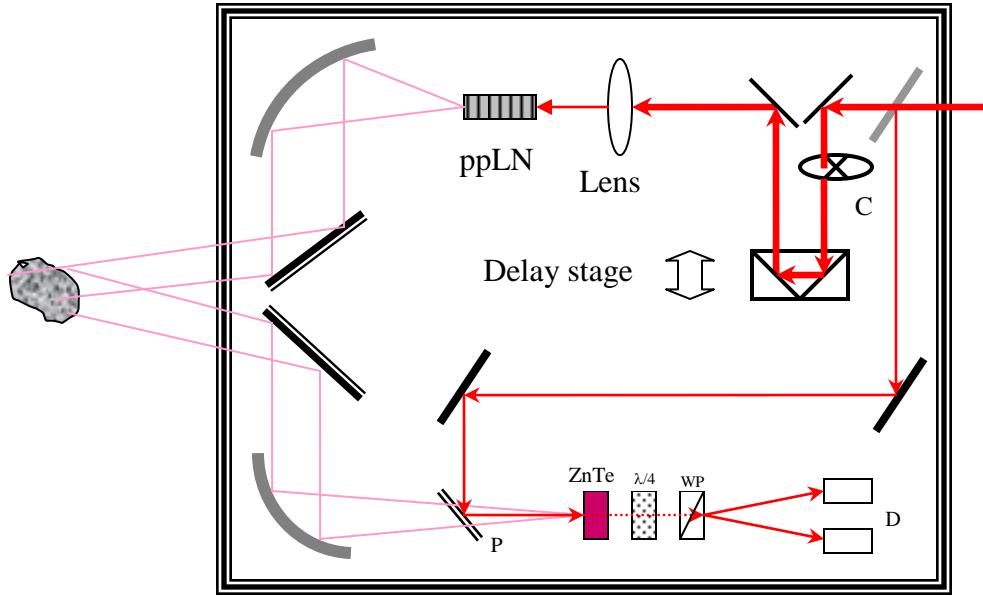


Fig. 6: Schematic diagram of a THz-TDS used in the THz range profile measurement. In the graph, C: optical chopper, P: pellicle membrane to reflect THz beam, $\lambda/4$, quarter wave plate, WP: Wollaston beam splitter, D: balanced detector.

Fig. 7 shows the expected electric field amplitude emitted from the AppLN crystal. The maxima are closer in time at the early end of the pulse than at the late end, indicating that the frequency is changing from high to low. Panel (b) of Fig. 7 shows the wavelength as a function of time; it has the characteristic “chirped” appearance that is sought for these experiments.

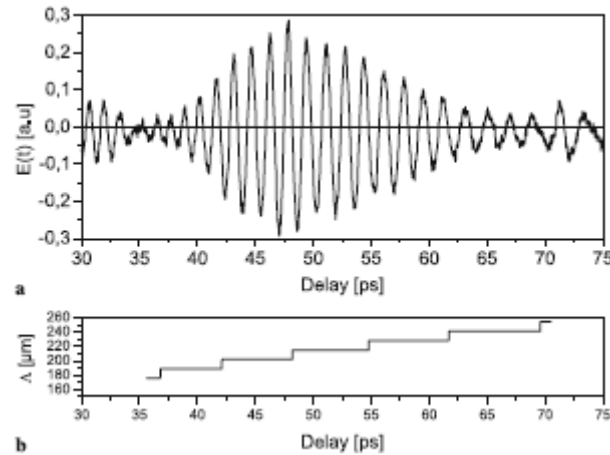


Fig. 7: Experimental electric field amplitude of AppLN sample comparable to those used in this work. (b) Corresponding wavelength dependence vs. time; the pulse is “chirped” as desired. Taken from Ref. 9.

We measured the signal as a function of delay stage position, which is analogous to delay time. Fig. 8 and Fig. 10 show the signal vs. delay position for Sample a and b, respectively, and Fig. 9 and Fig. 11 show the corresponding Fourier transform of those

signals, which give the frequency spectra. The inset in Fig. 8 shows the blow-up of the first few cycles of the waveform. The awkward turning corner is believed to be due to the inaccurate control of domain thickness, which doesn't affect the measurement. In Fig. 9, apart from the main lobe of 300-500GHz spectrum, there is a side peak located at about 1.4THz.

Comparing Fig. 9 and Fig. 11, clearly sample b has a frequency range. The Fourier spectrum shows a spectrum range of 0.5-1.5THz, narrower than the designed nominal range 0.5-5THz. This is due to the detector crystal, ZnTe, having a limited response range. The Fourier transform spectra look noisy, since the measurement was intentionally done in free space, in which the humidity would deteriorate the result; this was done to more closely replicate the realistic environment in which an eventual device would be utilized. Overall, we obtained a chirped THz spectrum that can be used for range profiling. Next, we used sample *b* to measure several target samples.

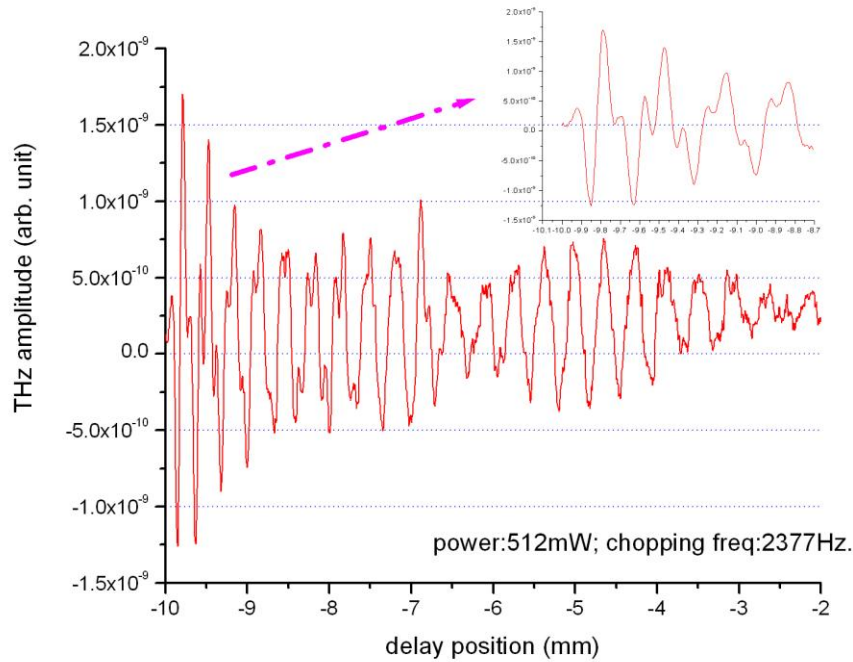


Fig. 8: Waveform for AppLN sample b, nominal frequency range: 300-500GHz.

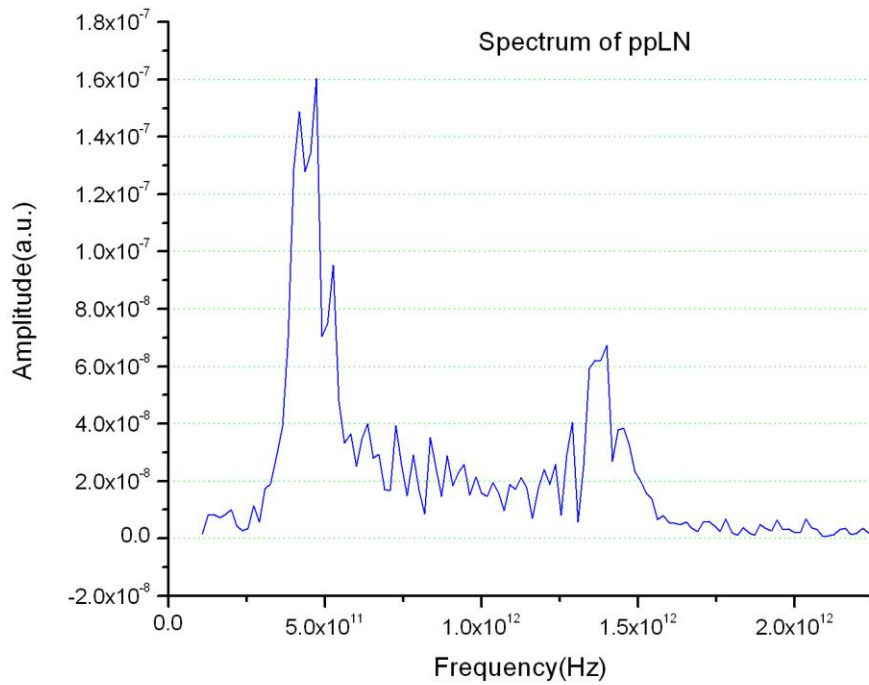


Fig. 9: FT spectrum of sample b. The DC component is removed.

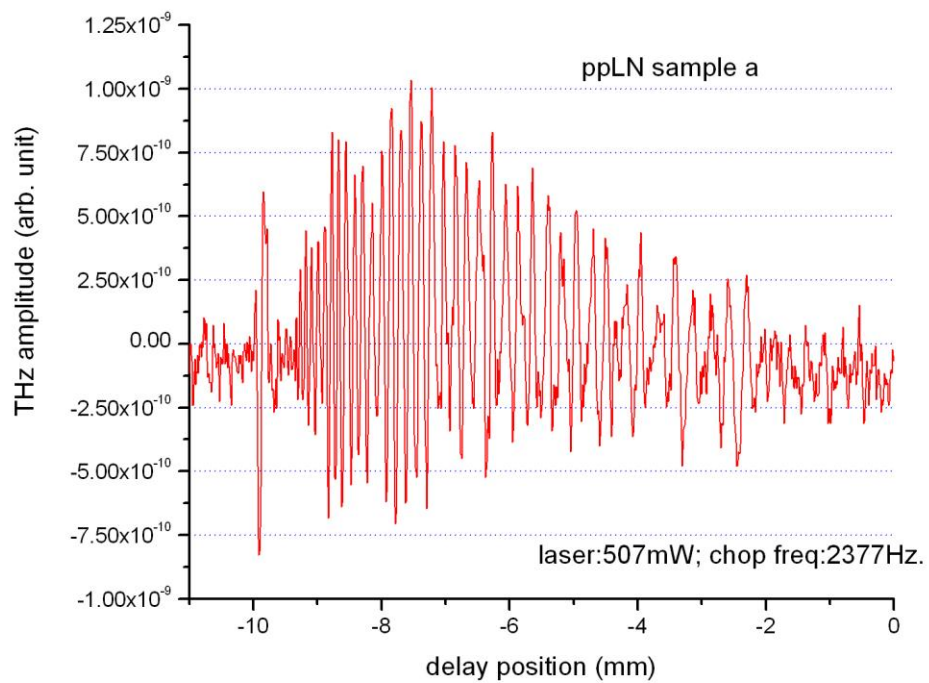


Fig. 10: Sample a waveform.

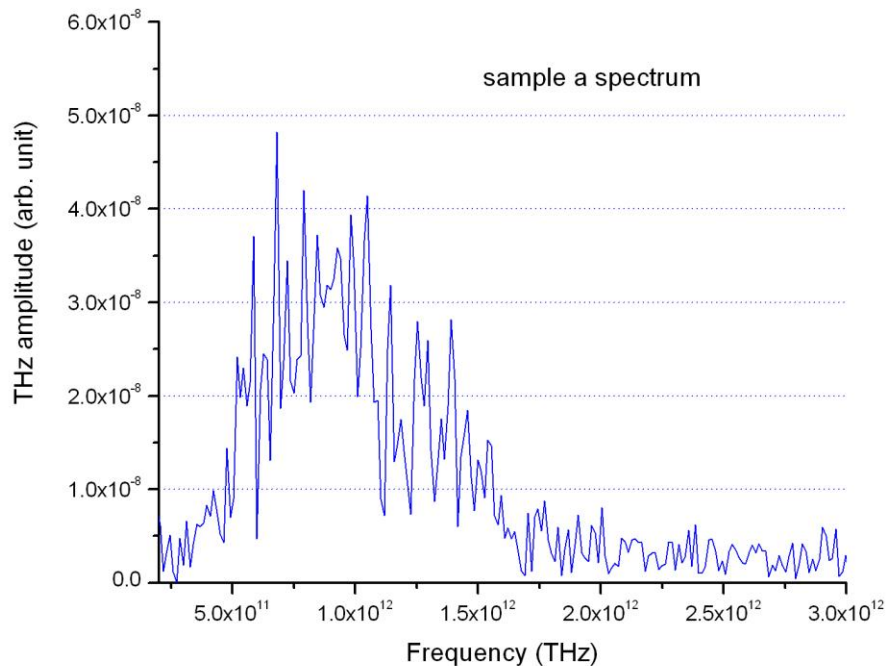


Fig. 11: Sample a spectrum. Note the cutoff at around 2THz. This is due to the ZnTe crystal, whose response is limited to this value.

All of the experiments performed in this study used metal samples. The samples were attached with double-stick tape onto the surface of a mirror. The THz beam was assumed to be 5 cm in diameter, and all of the targets were sufficiently small that the whole target was always fully inside the THz beam. The use of the mirror allowed those frequencies not strongly reflected by the target to nevertheless contribute to the overall spectrum, which facilitated comparison of the target signal intensity and location with respect to the delay axis.

Although the eventual goal of this work would be detection of targets of military significance, such as concealed weapons or IEDs, for this effort, a proof-of-concept was deemed appropriate. As such, the targets selected included common laboratory items of different shapes, including washers, hex nuts, and standard optics hardware. These objects have a finite thickness, which reduces the travel distance of the beam and should result in a signal earlier than the main AppLN waveform, but this is not observed, probably due to severe noise in the signal in this regime. All data in this work is presented in the temporal range corresponding to that of the reference signal from the AppLN reflected off of a mirror.

EXPERIMENTAL DATA

We first sought to establish that the reflected signal from a target can be distinguished from random noise. To this end, we measured the spectrum of a target five times to verify that the measurements were reproducible. The target used was a specially constructed Al “wedding cake”, with tiers approximately 6.4 mm high and 6.35 mm, 12.7, and 19 cm in diameter, respectively. A schematic of this “wedding cake” structure is shown in Fig. 12.

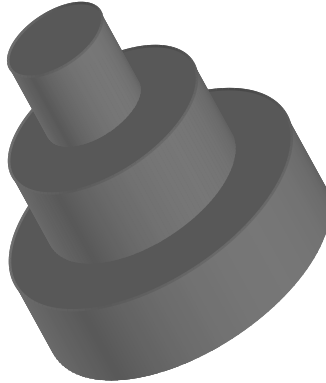


Fig. 12: "Wedding cake" sample schematic.

Fig. 13 shows the signal obtained from this sample using AppLN sample b in five separate runs. Note that the variations on the vertical axis are due to a run-to-run DC drift, and inherent to the data. The location and heights of the peaks are consistent from run to run. The inset shows the details of the first few cycles. Fig. 14 shows the average of all of these spectra with the reference signal from just the mirror. The maxima and minima in the wedding cake spectrum correspond with those of the reference spectrum.

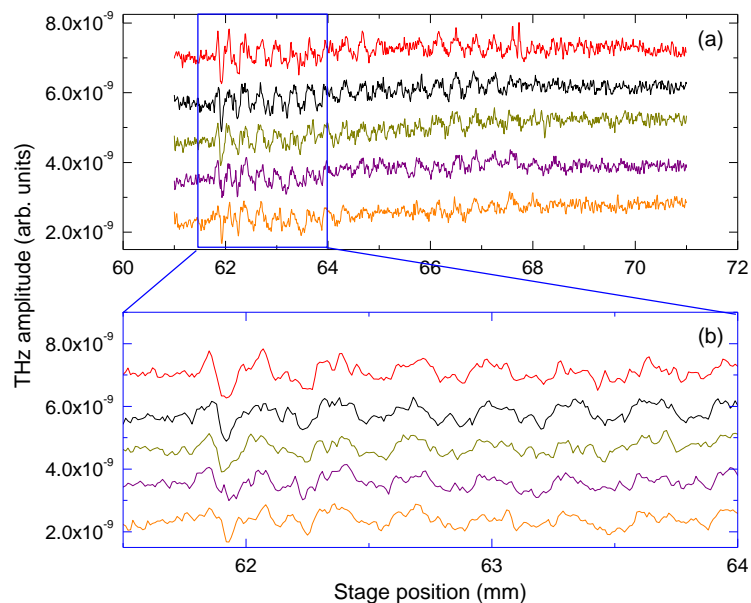


Fig. 13: 'Wedding cake' sample response. This graph indicates the reproducibility of the measurement. (a) shows data over the full range of the delay stage while (b) is zoomed in on the region from 61.5 to 64 mm. The data have been offset vertically for clarity.

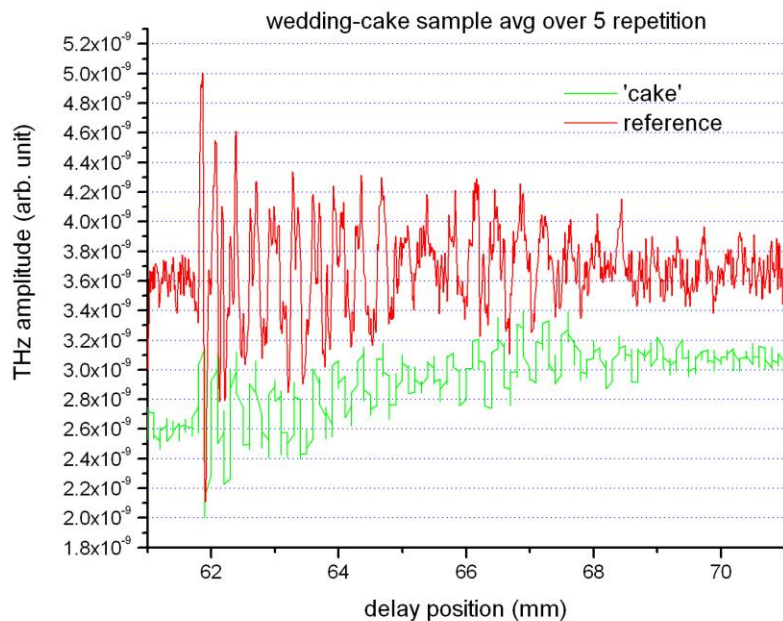


Fig. 14: Average response of 'wedding cake' sample, as compared to the reference signal.

The intent for these measurements is to determine whether the sample alters the THz waveform significantly enough that results from targets of different shapes or geometries could be expected to be discriminated. Considering the difference between the signal from the wedding cake sample and the reference signal, as shown in Fig. 15, the waveform intensity is nearly one order of magnitude smaller than that of a mirror, and the data exhibits quite sharp corners from data processing. This results in a low signal-to-noise ratio (S/N), which could present difficulties for discrimination of actual targets.

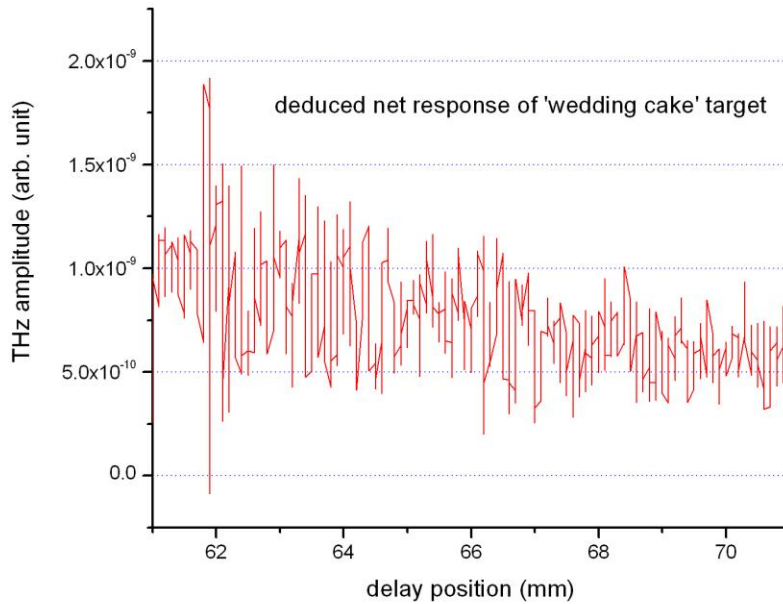


Fig. 15: Difference between "wedding cake" and reference signals, from Fig. 14.

Next, we tested other artificial targets, which consist of several arrangements of common objects. The first arrangement consists of an aluminum block and a washer. The second consists of a penny, nickel, and quarter, with faces roughly normal to the incident THz beam. The third target is a square metallic block with a few tapped holes. The fourth target consists of several hex nuts. The pictures of these combined samples are shown in Fig. 16.

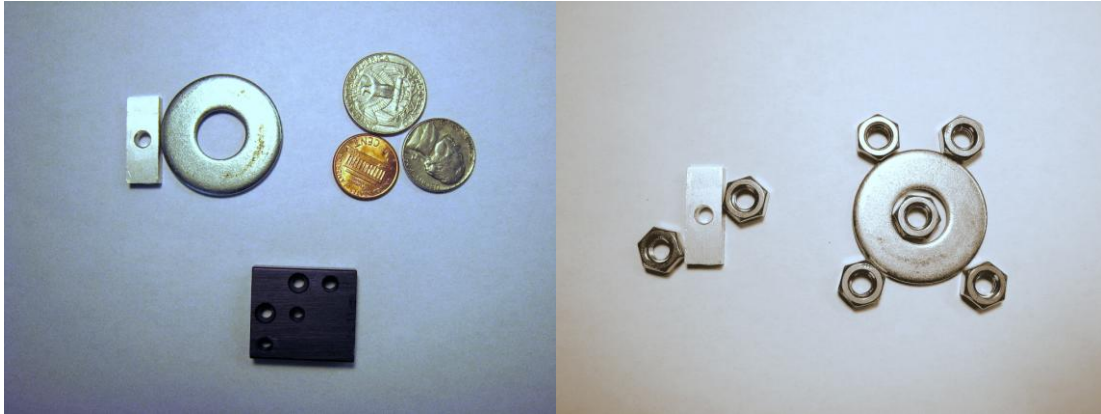


Fig. 16: Pictures of targets used in the experiments.

The purpose of these tests is to determine whether waveform features can be distinguished for these samples. Furthermore, an algorithm is developed to perform the convolution between the reflected waveform and that of the reference. This is essentially the operation of matched filter detection in radar and telecommunications.¹¹

The reference signal after matched-filter is shown in Fig. 17. The blue vertical line indicates the onset of the convolution, while the green line marks the peak, which corresponds to the actual delay stage location of the THz signal reflected by the mirror.

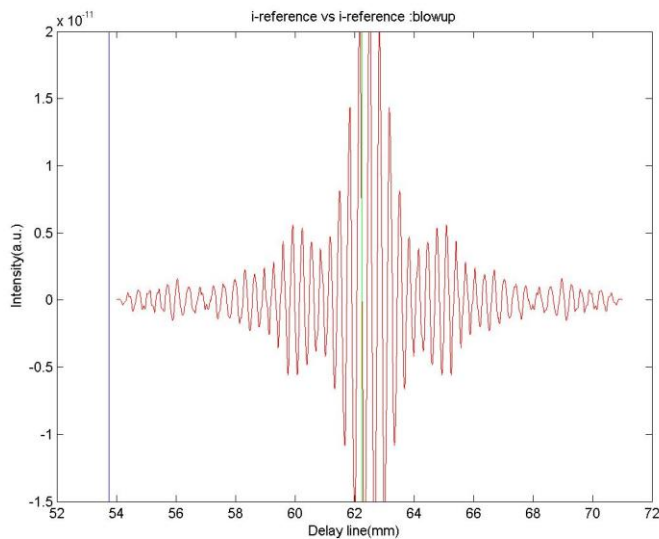


Fig. 17: Reference signal after matched-filter by itself.

Fig. 18 shows the result for the 'square block' target. The features of the waveform to the left of blue line are the contributions purely from the sample surface, while those between the two vertical lines are from both the sample and the mirror. The target's waveform is measured for two different orientations of the target. In both cases, the entire sample is contained within the THz beam. The two panels of Fig. 18 show similar features.

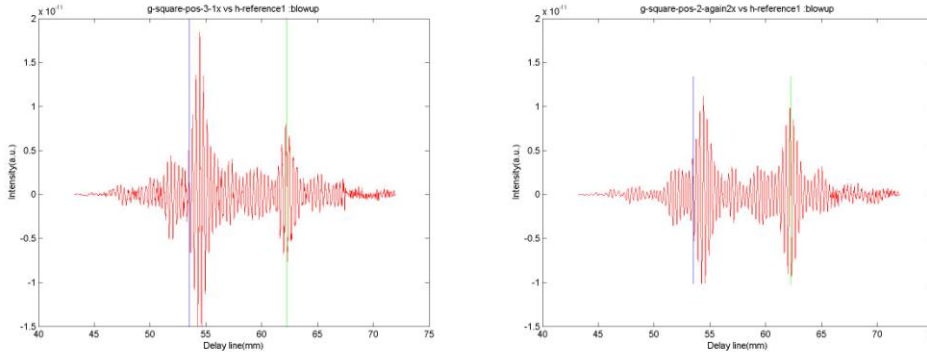


Fig. 18: Signal from sample 'Square block'.

Fig. 19 shows the result for sample 'Al block & washer'. Compared with that in Fig. 18, we see distinguishable waveform characteristics. However, the feature to the left of blue line is weak; this is due to that the reflection area of the sample is small compared with that of 'square block'. In future work, as the target size is increased and the THz beam is made correspondingly larger, more pronounced signal should be observed.

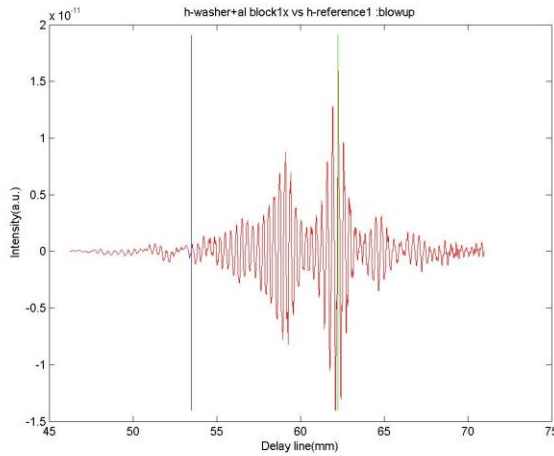


Fig. 19: Signal from sample 'Al block & washer'.

Next, we investigate the limit of THz beam resolution. Fig. 20 shows the waveform comparison between a washer sample and a randomly-arranged collection of 5 hex-nuts, taken separately. The plot only shows the portion to the left of the vertical blue line, as that in Fig. 19; the mirror contribution is excluded. The dimensions of the samples are marked on the plot, thickness by cross-section areas, indicating the possible contribution from samples due to their different thickness. It is clear the waveform envelope is different for different samples, even taking into account the delay time shift due to different thickness; the amplitude, however, relies on the cross section area.

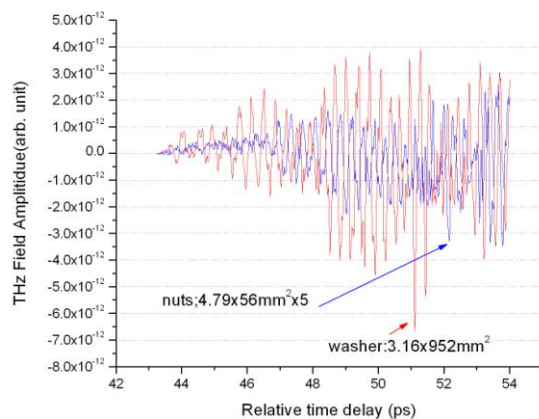


Fig. 20: Waveform comparison between two samples: a collection of hex nuts (blue waveform) and a washer (red waveform).

In Fig. 21, the signal for the 3-coin target is shown, after the matched filter. Fig. 22 shows the comparison of waveform between the 3-coins and reference, with the x-axis zoomed in on the region to the left of the blue line in Fig. 21. The dimensions of the penny, nickel and quarter, thickness by cross section, are marked based on their thickness and cross section. Compared with the result for the washer and hex nuts, the coins show no distinctive features, and the difference from the reference signal is also minimal.

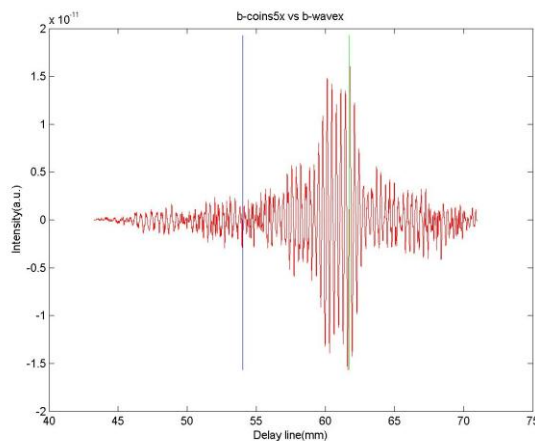


Fig. 21: Waveform of 3-coin target.

Reflection cross section area alone cannot explain why the difference is so small, since a penny's area, 284mm^2 , is comparable to that of 5-nuts, $56 \times 5 = 280\text{mm}^2$; see Fig. 20. The main reason is the signal diffraction on the embossed patterns of the coins. We measured the reflection from other metal and plastic surfaces that were topographically smooth but unpolished, and the reflected THz signal (not shown) was stronger than for the coin samples we measured.

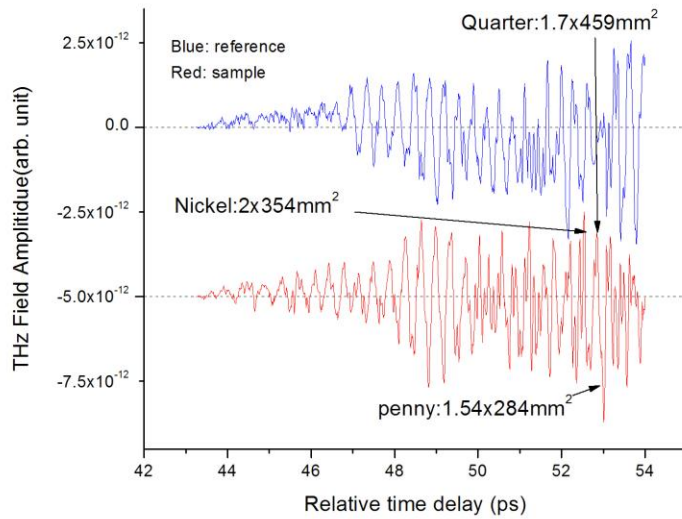


Fig. 22: Zoomed-in view of the 3-coin waveform of Fig. 21 for the region to the left of the blue vertical line. Data has been offset vertically for ease of viewing.

Based on the preceding results, we conclude that for the 0.5THz bandwidth chirped THz beam and associated detectors we employed, the smallest cross-section resolution is about 280mm^2 for smooth surface.

If three different samples are graphed together, we see the power and limit of THz range resolution, shown in Fig. 23. The graph is truncated and shown from the peak line to the left, to exclude signal that is only from the reference mirror.

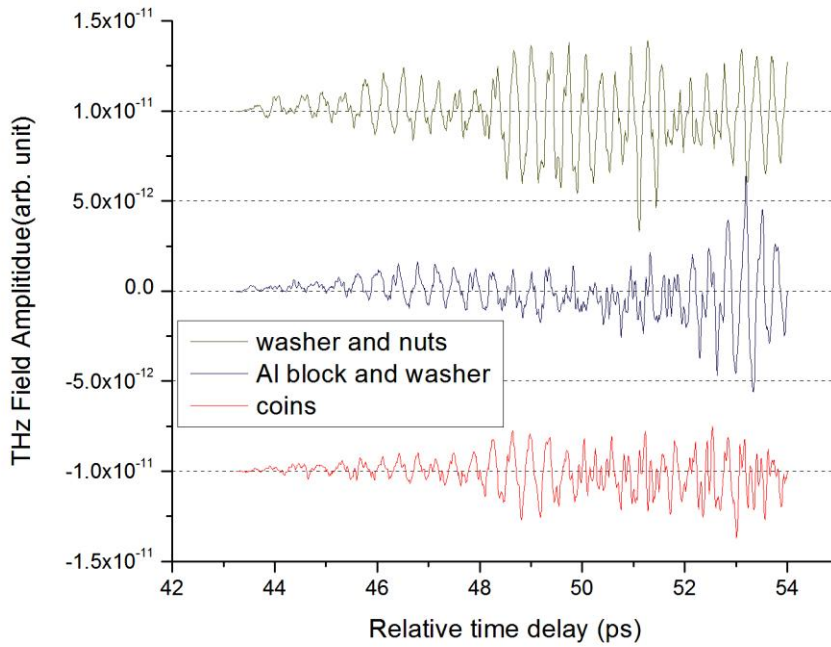


Fig. 23: 3-sample comparison. Data has been offset vertically for ease of viewing.

Fig. 23 shows different features of 3 different samples. Signals from ‘Al block & washer’ and ‘washer & nuts’ have quite different features, easily distinguishable from each other and from the reference signal. In contrast, as seen in Fig. 22, it is difficult to distinguish the coin signal from the reference. The target identification, however, could in principle be accomplished by a rigorous computing algorithm. Based on these preliminary results, advanced pattern recognition computer routines could be developed for machine training and target automatic identification. This could be accomplished, for example, by taking the peak values of each sample and projecting them into an n -dimensional Euclidean space and setting up a Mahalanobias classifier, which is one of the many criteria for pattern recognition.¹²

DISCUSSION

From the results in previous section, we conclude that THz radiation is capable of resolving small metallic targets. The smallest cross section is about 280mm^2 for smooth metal surface. Three different samples show distinguished time domain spectra that require no advanced pattern recognition algorithm for this phase of preliminary study. In these experiments, the targets were placed about 15cm away from the system, but the distance can be extended further to a distance of at least 1m without much difficulty. The eventual vision for the project would be the development of a database of the spectra generated for different targets with different aspect angles. Most likely, the database would monitor the amplitude of the peaks at each frequency. A computer algorithm would then be developed and trained for pattern recognition with high level of confidence.

Before reaching these considerations, however, further investigation on THz range profiling would need to address two significant technical challenges that have been identified during this project. The first pertains to the time required for the measurement. Since the THz waveform is on the order of tens of ps in time domain, the experiment employs a mechanical delay stage to obtain higher signal to noise ratio. For the range investigated in this work, the data acquisition took 10 minutes or longer. By replacing the delay stage with a fast continuously moving stage, it is possible to reduce the scan time within 2 seconds for about 10 cm target scan.¹³ In the meantime, a linear encoder is attached to the delay stage to monitor the movement. It sends out a TTL pulse to trigger fast data acquisition devices for every tiny distance, say 1 μm , the stage advances. A careful design could make it feasible to build a system that could scan a 15 cm within 5 seconds with acceptable S/N. Another solution, as discussed earlier, is to use a single-shot measurement scheme.^{2,3} This is a well-established technique without significant resolution decrease, but the system would require several additional components, including a spectrum analyzer, which makes it more expensive and complicated. As a result, this approach was not attempted during this effort. Nonetheless, it is difficult for single-shot scheme to cover more than 10cm scan range (300ps equivalently). A combination of mechanical delay and single-shot has to be employed to meet the requirement. This inescapably requires some time. Overall, the best performance for a THz range profiling device is estimated at the level of 10cm within 2 seconds. This is at the borderline of required specifications since we have not considered the movement of target yet. The scanning is only at fixed aspect angles. To summarize, an improvement in the scan time has to be made to lead to practical device.

Second, THz radiation power is generally weak (about 100nW) under laboratory conditions. To make this approach viable for field testing, for example, in a humid environment, at a standoff distance of 10-30 meters, either the THz radiation power needs to be increased to the mW level, or other highly sensitive detection devices have to be used (low temperature bolometer or passive antenna). This is a hurdle faced by any THz spectrometer application. Numerous research efforts have been devoted to this problem, with some signs of progress. One promising approach is the use of air plasma as a THz emitter and detector. This permits traversal of the long standoff distances to be achieved with visible and IR wavelengths, with the THz beam only being generated at a location arbitrarily close to the target.¹⁴⁻¹⁶ Further research could identify avenues for such a concept to be incorporated into this detection scheme.

CONCLUSION

A THz radiation range profile system is implemented to detect small targets at tens of centimeters standoff distance. The spatial resolution for the target is 1 millimeter in length and 280mm² in cross section for smooth metal surfaces. The measured range profiles demonstrate distinguishable waveform features for different samples. Due to the ps sampling time in THz detection against ms in radar, it takes minutes for the system to finish the range profile scanning, a technical hurdle that must be overcome as an essential element of further development. Additionally, the THz beam power needs to be upgraded to mW level for practical stand-off distance target identification.

ACKNOWLEDGEMENT

The authors gratefully acknowledge Prof. René Beigang of Technische Universitat Kaiserslautern, Germany, for providing the AppLN samples used in this study, and Albert Redo-Sanchez, Moayyed Hussain, Mark Doxbeck, Mark Johnson, Xu Xie and Tao Yuan for helpful discussions and technical assistance. This project was funded by an ARDEC TeXX grant.

REFERENCES

- ¹G.R. Curry, *Radar System Performance Modeling*. (Artech House, 2005).
- ²Z. Jiang and X.C. Zhang, *Opt. Lett* **23**, 1114 (1998).
- ³J. Shan, A.S. Weling, E. Knoesel, L. Bartels, M. Bonn, A. Nahata, G.A. Reider, and T.F. Heinz, *Opt. Lett* **25**, 426 (2000).
- ⁴D.R. Wehner, *High-Resolution Radar*. (Artech House, Boston, 1995).
- ⁵Q. Wu and X.C. Zhang, *Applied Physics Letters* **71**, 1285 (1997).
- ⁶J.A. L'Huillier, G. Torosyan, M. Theuer, Y. Avetisyan, and R. Beigang, *Applied Physics B: Lasers and Optics* **86**, 185 (2007).
- ⁷Y.S. Lee, *Applied Physics Letters* **77**, 2488 (2000).
- ⁸Y.S. Lee, T. Meade, T.B. Norris, and A. Galvanauskas, *Quantum Electronics and Laser Science Conference, 2001. QELS'01. Technical Digest. Summaries of Papers Presented at the 45* (2001).
- ⁹J.A. L'Huillier, G. Torosyan, M. Theuer, C. Rau, Y. Avetisyan, and R. Beigang, *Applied Physics B* **86**, 197 (2007).
- ¹⁰Y.S. Lee, *Applied Physics Letters* **82**, 170 (2003).
- ¹¹For example, see Henry Stark and John W. Woods, *Probability and Random Processes with Applications to Signal Processing* (2nd edition), (Prentice Hall, 2002).
- ¹²H. Zhong, "Terahertz Reflective Sensing and Imaging", Thesis, Rensselaer Polytechnic Institute, 2006.
- ¹³Zhang et al., (unpublished)
- ¹⁴X. Xie, J. Dai, M. Yamaguchi, and X.C. Zhang, *Proceedings of SPIE* **6212**, 62120N (2006).
- ¹⁵X. Xie, J. Dai, and X.C. Zhang, *Phys. Rev. Lett.* **96**, 75005 (2006).
- ¹⁶H. Zhong, N. Karpowicz, and X.C. Zhang, *Applied Physics Letters* **88**, 261103 (2006).